Mon. Not. R. astr. Soc. (1981) **196**, 1051–1066

Magnetohydrodynamic Kelvin–Helmholtz instabilities in astrophysics – II. Cylindrical boundary layer in vortex sheet approximation

A. Ferrari *Max-Planck-Institut für Extraterrestrische Physik, Garching b. München, Germany and Istituto di Cosmo-geofisica del CNR, Torino, Italy*

E. Trussoni and L. Zaninetti *Istituto di Cosmo-geofisica del CNR, and Istituto di Fisica Generale, Corso Massimo d'Azeglio 46, I-10125, Torino, Italy*

Received 1981 February 11; in original form 1980 November 11

Summary. This second paper of the series is devoted to Kelvin–Helmholtz instabilities in cylindrical boundary layer flows (jets). The vortex-sheet approximation is still used, and compressible flows are studied in subsonic, transonic, supersonic and relativistic regimes. Magnetic field effects are analysed, together with density contrast inside and outside the jet. The general result is that, due to the onset of a so-called reflection branch of resonant modes, jets are always unstable, both to pinching and helical perturbations with wavelengths of the order of the jet circumference. In particular the time-scales for instability are such that this certainly plays a significant part in the morphology and energetics of extended radio sources.

1 Introduction

High-resolution observations of extragalactic radio sources are providing interesting tests for theoretical models. They stress the basic fact that the energy supply is taking place continuously via directed flows and at the same time they confirm that *in situ* re-acceleration of relativistic electrons is needed for synchroton emission over extended regions. In addition, detection of well-collimated jets within 1 pc from parent galactic cores puts limits on the interaction between matter directionally expelled and the surrounding intergalactic medium.

In this context some authors (Ferrari, Trussoni & Zaninetti 1978; Hardee 1979) have discussed apparent morphological structures in terms of Kelvin–Helmholtz instabilities at the interface of fluid beams with an external (confining) medium. For instance Kelvin–Helmholtz instabilities appear to be capable of producing distortions of beams over scale lengths comparable to those actually observed. On the other hand, it has also been argued that unstable short-wavelength perturbations could produce scatterings to accelerate *in situ* relativistic electrons along the beam (Ferrari, Trussoni & Zaninetti 1979; Eilek 1979).

These proposals require a detailed knowledge of the physics of Kelvin–Helmholtz instabilities, specifically for the case of supersonic compressible flows in cylindrical geometry. In fact the introduction of a finite transverse dimension, namely beam radius, is necessary to discuss perturbations on scales comparable with those observed. Some results have already been derived for hydrodynamical and MHD flows from the asymptotic approximations to the linear dispersion relation, and two classes of modes must be considered:

(i) pinching modes, azimuthally symmetric;
(ii) helical and fluting modes, with azimuthal dependence.

In the case of hydrodynamical flows, the solutions (Gill 1965; Lessen, Fox & Zien 1965; Ferrari *et al.* 1978; Hardee 1979) show the following pattern (k is the perturbation wavenumber, a the beam radius):

(a) long-wavelength perturbations, $ka \ll 1$, can always be unstable for large enough angles of propagation with respect to the beam velocity, i.e. for modes with large azimuthal wavenumber. Pinching modes have growth rates typically lower than helical or fluting modes;

(b) for short wavelengths, $ka \gg 1$, the dispersion relation converges to that for the plane vortex-sheet case for flows with Mach numbers below the critical cut-off Mach number, M_c ($=\sqrt{8}$ for equal fluids). For faster flows some authors (Gill 1965; Lessen *et al.* 1965) had remarked that new unstable modes could arise at short wavelengths, but they were not investigated in detail.

MHD flows have been studied numerically by Chakraborty & Iyengar (1975, 1977), Ershkovich & Heller (1977) and Ray (1981), mainly for long and intermediate wavelengths, $ka \lesssim 1$. They showed that the presence of longitudinal magnetic fields increases the growth rate of helical modes, although sub-Alfvénic flows are always stable both to pinching and helical perturbations.

This paper, which follows a previous one where the plane vortex-sheet case was treated (Ferrari, Trussoni & Zaninetti 1980: Paper I), presents a study of the (linear) Kelvin–Helmholtz instability for the case of flowing jets with cylindrical boundaries. Again the vortex-sheet approximation is used, referring to a subsequent paper for the analysis of sheared boundary layers. In Section 2 the basic set of equations is given, and asymptotic limits ($ka \gg 1$ and $ka \ll 1$) are derived as a guide for the numerical work. Then in Section 3 we illustrate the numerical solution of the linear dispersion relation for the intermediate case $ka \sim 0.1 - 10$ for which the asymptotic approximations are not valid; in particular the new class of unstable modes in supersonic flows ($M \gtrsim 2$), preliminarily indicated by Gill (1965) and Lessen *et al.* (1965), is studied in detail, showing that it has strong growth rates and disappears only when $ka \to \infty$. In the final Section these results are confronted with the models for radio jets. The new unstable modes for supercritical flow speeds are shown to be crucial in that astrophysical framework, as they may have very large growth rates. A tentative extrapolation to the non-linear regime is also suggested in connection with magnetospheric data.

2 General dispersion relation and asymptotic solutions

The basic set of MHD equations was discussed in Paper I, in connection also with its extension to the relativistic regime. In the present paper the same set of equations is used to study the Kelvin–Helmholtz instability of a flow axisymmetric along the z-axis. The equilibrium flow velocity is constant inside the jet and falls abruptly to zero at a radial distance a from the axis (cylindrical vortex sheet). An equilibrium magnetic field is considered, inside and outside the jet, parallel to the flow; transverse (azimuthal) fields can be discussed only for simple configurations, as their inclusion does not generally lead to an analytic dispersion relation. The typical perturbation is written as

$$f(r, \theta, z, t) = g(r) \exp\{i(kz + n\theta - \omega t)\}, \tag{1}$$

where n is called the azimuthal wavenumber ($n = 0, 1, 2 \ldots$). Assuming pressure equilibrium at the discontinuity surface, and expressing $g(r)$ in terms of Bessel and Hankel functions inside and outside the jet respectively, the following dispersion relation is obtained:

$$\frac{J_n'(ka\Delta_i)H_n^{(1)}(ka\Delta_e)}{J_n(ka\Delta_i)H_n'^{(1)}(ka\Delta_e)} = \nu_0\frac{\Delta_e}{\Delta_i}\,\frac{\gamma_0^2(M-\phi)^2-\mu^2}{\phi^2-\sigma^2/\epsilon^2}, \tag{2}$$

where J_n and $H_n^{(1)}$ are Bessel and Hankel functions of nth order; the primes indicate derivatives with respect to the arguments; U_0, V_A, V_S are the flow, Alfvén and sound velocities respectively, the subscripts 'e' and 'i' refer to the external medium and the jet, and

$$\gamma_0 = (1-\beta^2)^{-1/2} = \left(1-\frac{U_0^2}{c^2}\right)^{-1/2}, \quad M = \frac{U_0}{V_{si}}, \quad \phi = \frac{\omega}{kV_{si}},$$

$$\Omega = M - \phi, \quad \eta = \frac{\beta^2}{M}\phi - 1,$$

$$\nu_0 = \frac{\rho_{0i}^*}{\rho_{0e}^*}, \quad \rho_{0e,i}^* = \rho_{0e,i} + \frac{P_{0e,i}}{c^2}$$

$$\Delta_e^2 = \frac{\epsilon^2\phi^4}{\phi^2+\sigma^2/\epsilon^2(\epsilon^2\phi^2-1)} - 1$$

$$\Delta_i^2 = \frac{1+\eta+\Lambda_1}{1+\Lambda_2} - 1 \tag{3}$$

$$\epsilon^2 = \left(\frac{V_{si}}{V_{se}}\right)^2, \quad \mu^2 = \left(\frac{V_{Ai}}{V_{si}}\right)^2, \quad \sigma^2 = \left(\frac{V_{Ae}}{V_{se}}\right)^2,$$

$$\Lambda_1 = \frac{-\gamma_0^2\Omega}{\gamma_0^2\Omega^2-\mu^2}\left\{\mu^2\frac{\beta^2}{M}\eta - \Omega\left[\gamma_0^2\Omega\left(\Omega+\frac{\beta^2}{M}\eta\right)-\mu^2\right]\right\},$$

$$\Lambda_2 = \frac{\mu^2}{\Omega(\gamma_0^2\Omega^2-\mu^2)}\left\{\frac{\eta}{\gamma_0^2\Omega}\left[\gamma_0^2\Omega^2-\mu^2\left(1+\gamma_0^2\Omega\frac{\beta^2}{M}\right)\right]+\Omega\left[\gamma_0^2\Omega\left(\Omega+\frac{\beta^2}{M}\eta\right)-\mu^2\right]\right\}.$$

J_n and $H_n^{(1)}$ correspond to solutions for specific azimuthal wavenumbers: $n = 0$ solutions are usually called pinching modes, $n = 1$ helical or kink modes, and $n \geq 2$ fluting modes. It is straightforward to show that for $B_0 = 0$, i.e. $V_A = 0$, the dispersion relation (2) reduces to the purely hydrodynamical case discussed in Ferrari *et al.* (1978). Equations (2) and (3) must be solved for the non-dimensional complex phase velocity ϕ, with unstable modes corresponding to $\mathrm{Im}\,\phi > 0$. Before analysing the general solution of the dispersion relation, we derive its asymptotic limits, in terms of expansions of J_n and $H_n^{(1)}$.

For $n \neq 0$ and long-wavelength modes,

$$\left|\frac{n}{ka\Delta_i}\right| \gg 1, \quad \left|\frac{n}{ka\Delta_e}\right| \gg 1. \tag{4}$$

Equation (2) has an algebraic solution:

$$\phi = \frac{M\gamma_0^2\nu_0 \pm \nu_0^{1/2}\{(1+\nu_0\gamma_0^2)(\mu^2+\sigma^2)-\gamma_0^2M^2\}^{1/2}}{1+\nu_0\gamma_0^2} \tag{5}$$

and unstable modes exist only for

$$M^2 > (\gamma_0^2)^{-1}(1+\nu_0\gamma_0^2)(\mu^2+\sigma^2). \tag{6}$$

Obviously this result applies to helical or fluting modes only; it agrees with solutions for the plane vortex-sheet case, in the sense that any wavelength for n large enough (i.e. wavevector sufficiently oblique with respect to the relative velocity) can be unstable if the flow Mach number is larger than $\sim 2\, V_A/V_S$ (see Paper I).

In the case of short-wavelength modes,

$$\left|\frac{n}{ka\,\Delta_i}\right| < 1, \quad \left|\frac{n}{ka\,\Delta_e}\right| < 1, \tag{7}$$

the dispersion relation becomes multivalued:

$$\exp\left\{2i\left(ka\,\Delta_i - \frac{2n+1}{4}\pi - N\pi\right)\right\} = \frac{1+F_1(\phi)}{1+F_2(\phi)}, \tag{8}$$

where N is zero or any positive integer, and F_1, F_2 are regular analytic functions. In particular, sub-Alfvénic flows are stable and a cut-off Mach number exists for instability, as far as ka is not going to infinity; in addition, more unstable solutions are possible for any set of physical parameters, a feature typical of the general problem, as we discuss below. The asymptotic limits (5) and (8) provide checks for the numerical solutions of the following section. In fact the indeterminacy in sign of Δ_i, Δ_e in the arguments of $H_n^{(1)}$ and J_n could lead to unphysical solutions; namely, in accordance with the fact that $H_n^{(1)}$ gives the radial perturbation behaviour, one has to choose the sign of Δ_e in such a way that it fits with the limit given by (8), i.e. that its imaginary part is positive. Correspondingly we do not discuss here at length the implications of (5) and (8), as they are explored later, together with the general solution.

A last remark must concern the effect of an azimuthal magnetic field component in the jet; then an analytic dispersion relation can be derived for pinching modes only. An equation is obtained analogous to equation (2), where on the right-hand side the terms μ^2 and σ^2 are put to zero, and different scalings of the following parameters are used:

$$\phi = \frac{\omega}{k(V_{Ai}^2 + V_{Si}^2)^{1/2}}, \quad M = \frac{U_0}{(V_{Ai}^2 + V_{Si}^2)^{1/2}}, \quad c^2 = \frac{V_{Ai}^2 + V_{Si}^2}{V_{Ae}^2 + V_{Se}^2} \tag{9}$$

(V_A is defined in terms of the total magnetic field).

3 Analysis of the general dispersion relation

The solution of equation (2) had to be studied numerically in the intermediate range of values of ka, i.e. $0.1 \lesssim ka \lesssim 10$, for which the asymptotic limits previously discussed do not apply. In addition, only pinching and helical modes need to be calculated, as for larger azimuthal numbers equation (5) provides the trend of solutions.

The eigenmodes of the dispersion equation have been obtained by solving (2) for the real and imaginary parts of the complex phase velocity ϕ by means of suitably modified IBM subroutines for complex roots of analytical equations. In Figs 1–4 we plot $\mathrm{Re}\,\phi$ (dashed lines) and $\mathrm{Im}\,\phi$ (full lines) separately; $\mathrm{Re}\,\phi$ gives the eigenfrequency of oscillations, $\mathrm{Im}\,\phi > 0$ means that eigenmodes are unstable. Most plots are for ϕ versus ka for fixed Mach numbers and magnetic fields. In the following, we illustrate the behaviour of transonic, supersonic and eventually relativistic jets against Kelvin–Helmholtz MHD instabilities.

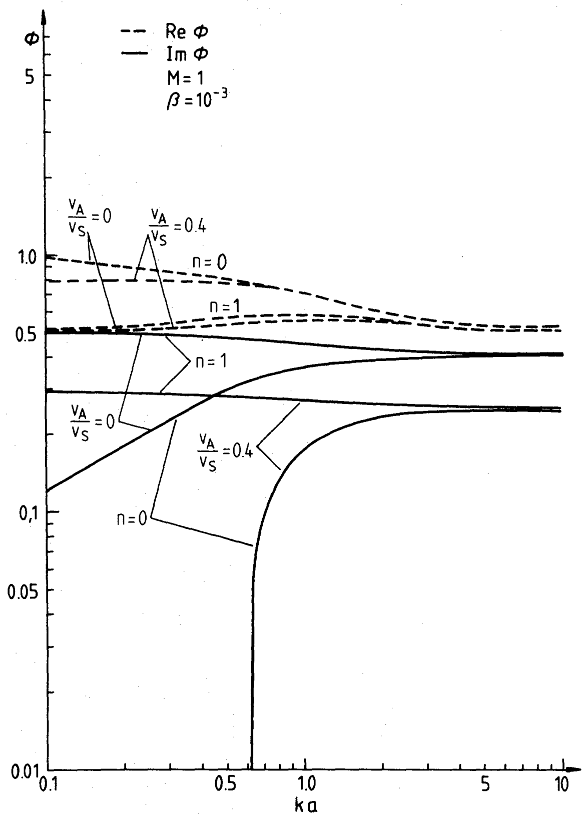

Figure 1. Complex non-dimensional phase velocity of unstable modes versus mode wavenumber for transonic flows and equal physical properties inside and outside the jet. Re ϕ (dashed lines) provide the oscillation frequency, Im ϕ (full lines) the mode growth rate. Results refer to pinching modes (n = 0) and helical modes (n = 1) for two values of V_A/V_S. Modes are stable for $V_A/V_S \gtrsim 0.5$.

3.1 SUBSONIC AND TRANSONIC FLOWS; EQUAL PHYSICAL PROPERTIES INSIDE AND OUTSIDE THE JET, LONGITUDINAL MAGNETIC FIELDS

As already indicated by the analytical limit (6), and in agreement with the plane boundary case of Paper I, all modes are stable for sub-Alfvénic flows. Then Fig. 1 shows that instability is always present for $M \gtrsim 2\, V_A/V_S$, apart from the large-wavelength pinching modes ($ka \ll 1$) that become stable. Results are given for $V_A/V_S < 0.5$; the pinching mode cut-off comes at larger values of ka for larger V_A/V_S.

3.2 SUPERSONIC FLOWS; EQUAL PHYSICAL PROPERTIES INSIDE AND OUTSIDE THE JET

In the plane vortex-sheet scheme, supersonic flows, $M \gtrsim \sqrt{8}$, are unstable only to modes with wavevector transverse to the relative velocity. As discussed in Paper I, this is due to lack of causal relationship when the relative velocity is much higher than the signal velocity, i.e. sound or Alfvén speed. For oblique modes the effective relative velocity is just the projection of the real velocity along their wavevectors, and then may be subsonic or transonic.

Now, for the jet configuration, pinching modes correspond to wavevectors parallel to the flow speed, helical and fluting modes to wavevectors winding up on the cylindrical surface. In fact, in the range $ka > 1$, we find consistently that the ordinary pinching and helical modes have very low growth rates; while instability can always be present for n large

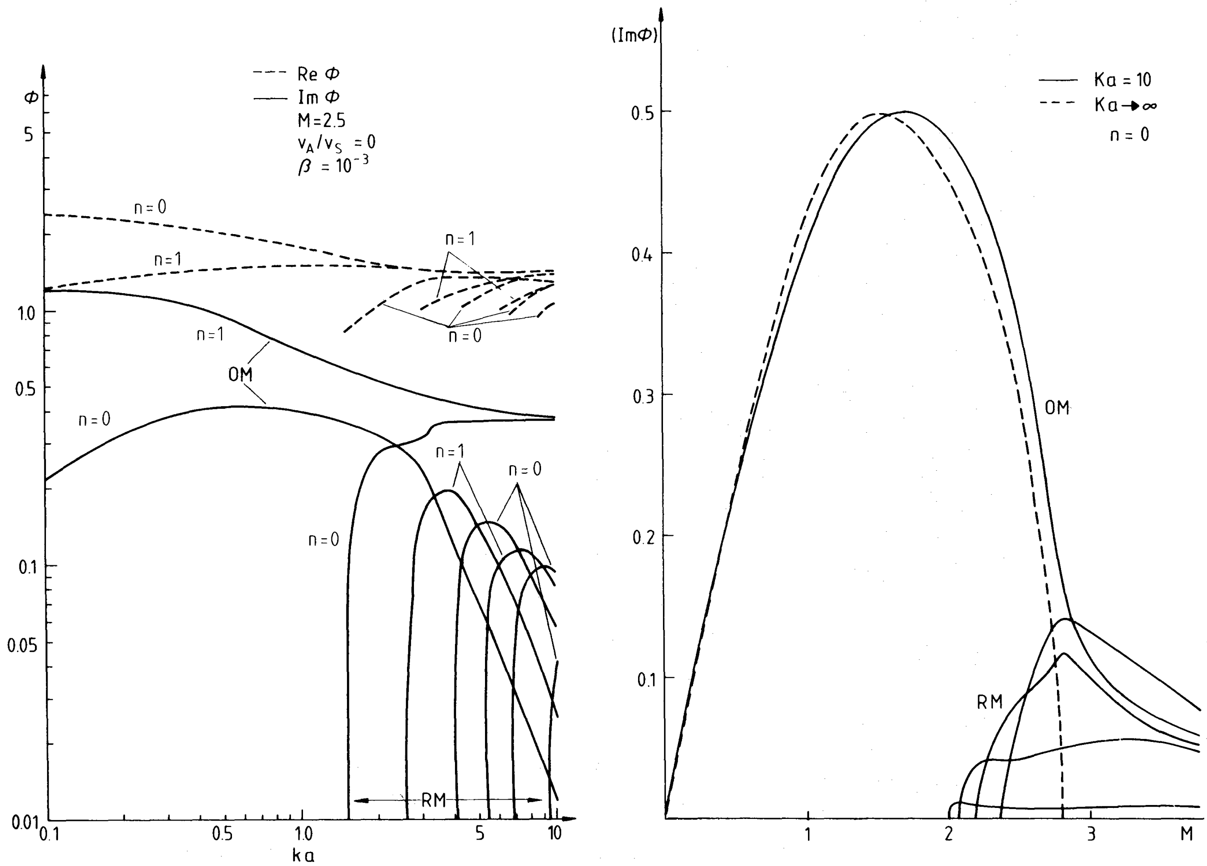

(a) (b)

Figure 2. (a) Complex non-dimensional phase velocity versus mode wavenumber for mildly supersonic flows and equal physical properties inside and outside the jet. OM refer to ordinary modes, RM to reflection modes. (b) Growth rates of unstable pinching modes versus transonic Mach numbers. Comparison of plane boundary results (dashed lines) with cylindrical boundary results (full lines), showing the onset of RMs.

enough, in agreement with equation (5) (see Figs 2a and 3a–f). Obviously, for long wavelengths, $ka < 1$, the plane boundary arguments do not apply, as transmission effects across the jet also come into play; they provide some correlation that still supports the instability, even for pinching modes. In this connection, at least for $n \neq 0$, the asymptotic solutions (5) and (8) predict instability at long wavelengths. Consistently, Figs 2 and 3 show that for $ka < 1$ and $M \gtrsim 2\, V_A/V_S$, both helical and pinching modes are unstable, but helical modes have much faster growth rates.

However, boundary effects are also relevant for short wavelengths, $ka > 1$, in the supersonic regime, as instability is actually increased by the onset of a new branch of modes (called reflection modes, RM, in the figures). This branch is present both for pinching and helical or fluting modes, has faster growth rates than ordinary modes (OM), and extends to larger wavelengths for faster flows. Its origin has to be related to the effects of mode reflection on the jet boundaries, that can resonantly excite marginally stable solutions (see, e.g. Miles 1957; Gill 1965). The range of frequencies of these unstable resonances is typically given by

$$1 \lesssim \mathrm{Re}\,\phi \lesssim (M-1), \qquad (10)$$

and therefore the number of new modes increases with the flow speed; this is clearly illustrated in Fig. 2(b) for $n = 0$. It is also interesting to note from the dashed curves of Fig. 3

that, while the ordinary branch has $\mathrm{Re}\,\phi \sim M/2$, the new RMs correspond at their onset to lower $\mathrm{Re}\,\phi$ which, for increasing ka, tend rapidly to reach the asymptotic limit (8). One sees from the numerical results that, as soon as the first RM growth rate overcomes that of the OM and reaches its maximum, a second RM appears and so on, with a regular spacing in ka. Altogether these RMs generate an envelope which follows the asymptotic behaviour of the OMs, but correspond to faster growth rates if $M \gtrsim 5$.

The RMs are especially important for pinching perturbations, that otherwise would be stable at short wavelengths in the presence of strong magnetic fields. Concerning the range of ka covered by RMs, one sees from Fig. 3 that it extends down to $ka \sim 0.5$ for $V_A/V_S \lesssim 3$ in the case of flows $M = 10$; by increasing M further, the new branch can reach the range of $ka \lesssim 0.1$.

3.3 RELATIVISTIC FLOWS

As discussed in Paper I, relativistic jets are more stable with respect to ordinary modes (see Fig. 4a, b), and especially to pinching modes (compare Figs 3b and 4a). Conversely, the reflection modes are not substantially affected, and maintain their maximum growth rates unaltered; this maximum is reached, however, at lower ka for increasing β, yielding small growth rates at large ka. Therefore, for ultrarelativistic flows ($\beta \to 1$), stability is expected, as OMs disappear and RMs are shifted to $ka \to 0$ (these always have slow growth rates in real physical dimensions, as $\mathrm{Im}\,\omega = ka\,\mathrm{Im}\,\phi \to 0$). Conversely, mildly relativistic jets are unstable at all wavelengths, for both $n = 0$ and $n = 1$, in the supersonic (and super-Alfvénic) regime.

3.4 MAGNETIC FIELD EFFECTS

They have already been discussed in connection with the instability cut-off for flow speeds below the Alfvén speed. Here we indicate a few additional points. Referring to longitudinal fields, $\mathbf{B}_0 \| \mathbf{U}_0$, a different behaviour has been found in pinching and helical OMs for flows $M \gtrsim 2.5$:

(i) for $n = 0$, instability is present up to magnetic field amplitudes such that $V_A/V_S \sim M$, but the growth rates become very small;

(ii) for $n \geq 1$, instability disappears already at $V_A/V_S \sim M/2$, but growth rates are correspondingly much higher. For RMs, the instability does not depend on n; an increase of field amplitude shifts the onset of the new branch to larger ka. Therefore strong magnetic fields tend to stabilize essentially long-wavelength pinching modes.

Concerning the presence of an azimuthal field component B_θ, we limit our discussion to pinching modes (see end of Section 2). This component has a destabilizing effect in general; for the same total amplitude $B = (B_\|^2 + B_\theta^2)^{1/2}$, growth rates are larger and the range of instability is fixed by $B_\|$ only. In particular, for a purely azimuthal field ($B_\| = 0$), previous results for $V_A/V_S = 0$ apply, when the scaling laws (9) are used for quantitative estimates: these indicate that no cut-off of instability exists for any value of M. Concerning $n \neq 0$ modes, one can only refer to the results for the plane vortex-sheet case with $R > 0$, which apply to short wavelengths, $ka \to \infty$.

3.5 DIFFERENT PHYSICAL PROPERTIES INSIDE AND OUTSIDE THE JET

We have studied the effect of contrasts of density and magnetic field amplitude. For unmagnetized fluids it is known (Ferrari *et al.* 1978) that the fastest growing modes are obtained

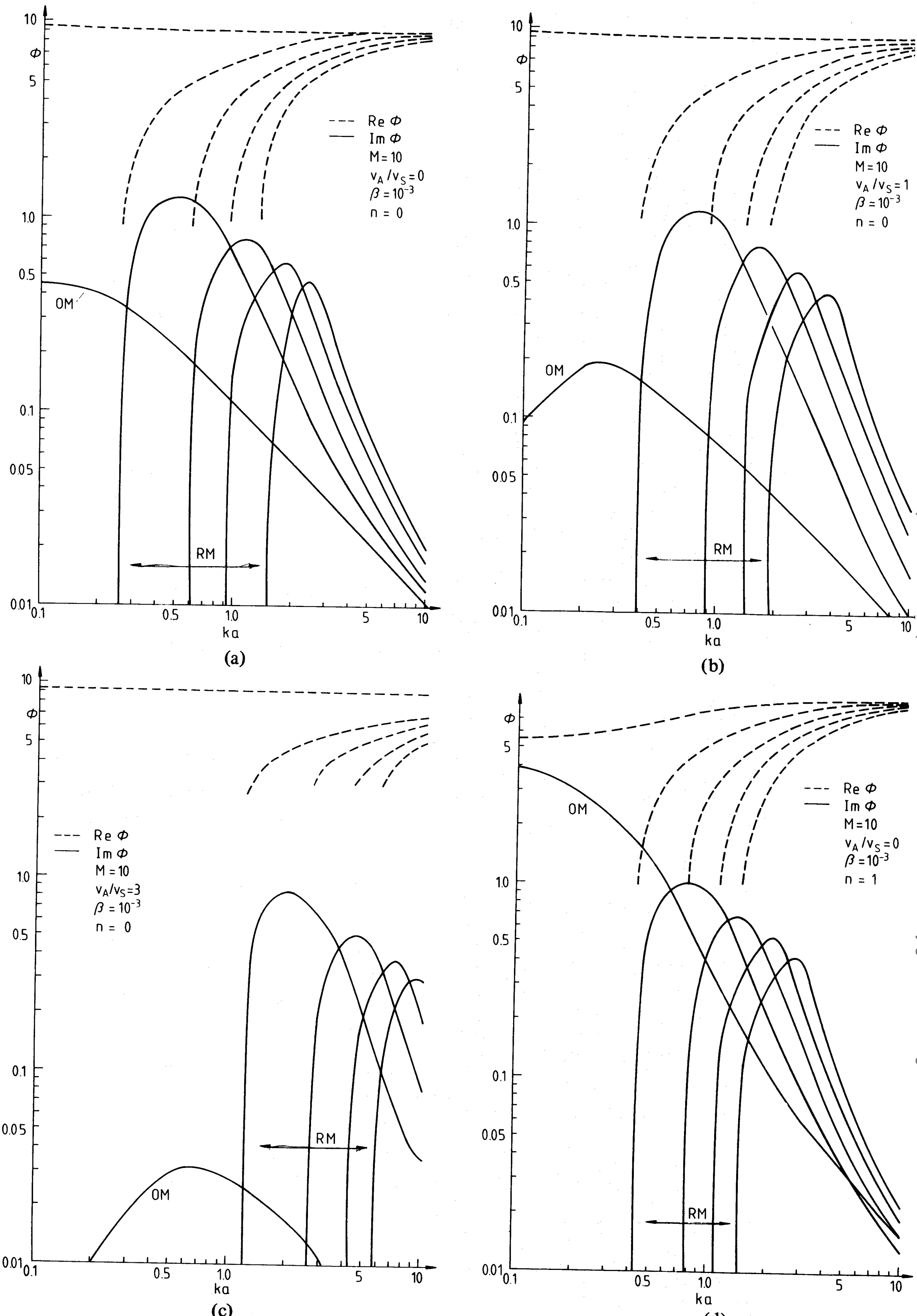

Figure 3. (a)–(c) Re ϕ and Im ϕ versus ka for unstable pinching modes in supersonic flows for increasing values of the magnetic field amplitude, V_A/V_S, with $\mathbf{B}_0 \| \mathbf{U}_0$. Pinching modes become stable for $V_A/V_S = M$. (d)–(f) Re ϕ and Im ϕ versus ka of helical modes in supersonic flows for increasing values of the magnetic field amplitude, V_A/V_S, with $\mathbf{B}_0 \| \mathbf{U}_0$. Helical modes become stable for $V_A/V_S = M/2$.

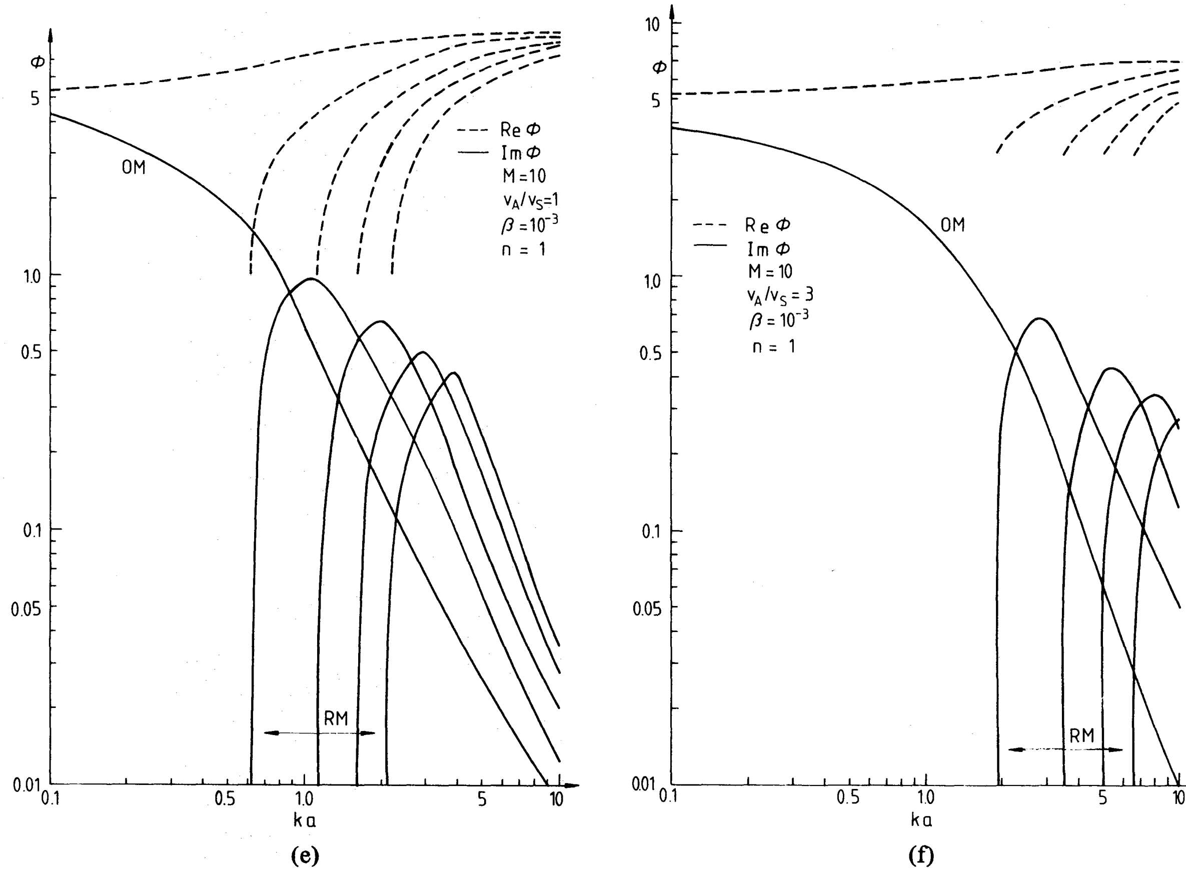

Figure 3 – *continued*

for equal fluids, in the jet and outside. Correspondingly one obtains stability for $\nu_0 \ll 1$ or $\gg 1$.

When considering short wavelengths, the results always approach those of the plane vortex-sheet case; the growth rates are similar for symmetrical values of the density contrast with respect to $\nu_0 = 1$. Light jets and heavy jets behave similarly for short wavelength perturbations.

For intermediate and long wavelengths, the situation is complicated by the presence of reflection modes. These are shifted towards larger (or smaller) ka when increasing (or decreasing) ν_0 around unity. However, the overall effect is always that of lowering the growth rates, so that the situation is again more or less symmetrical. The same is true when introducing discontinuities of the magnetic field strength at the beam surface while maintaining a total pressure equilibrium. As expected, the lowest growth rates are for $B_e:B_i = 1$.

The cumulative effects of magnetic field and density contrasts are illustrated in Fig 4(c), (d). One notices that all modes, but especially OMs, are stabilized, in the sense that growth rates decrease and the range of V_A/V_S for instability is narrowed.

3.6 TYPICAL MODE FREQUENCIES AND GROWTH RATES

We want to re-examine the results of Figs 1–4 from a general point of view. The typical oscillation frequencies for OMs are (apart from some numerical factors depending on n and ka) $\omega \sim 2(ka) \cdot M/\tau_c$, where $\tau_c = 2a/V_S$ is the jet crossing-time for sonic perturbations. For RMs, frequencies are smaller at long wavelengths, and approach those of OMs for $ka < 1$.

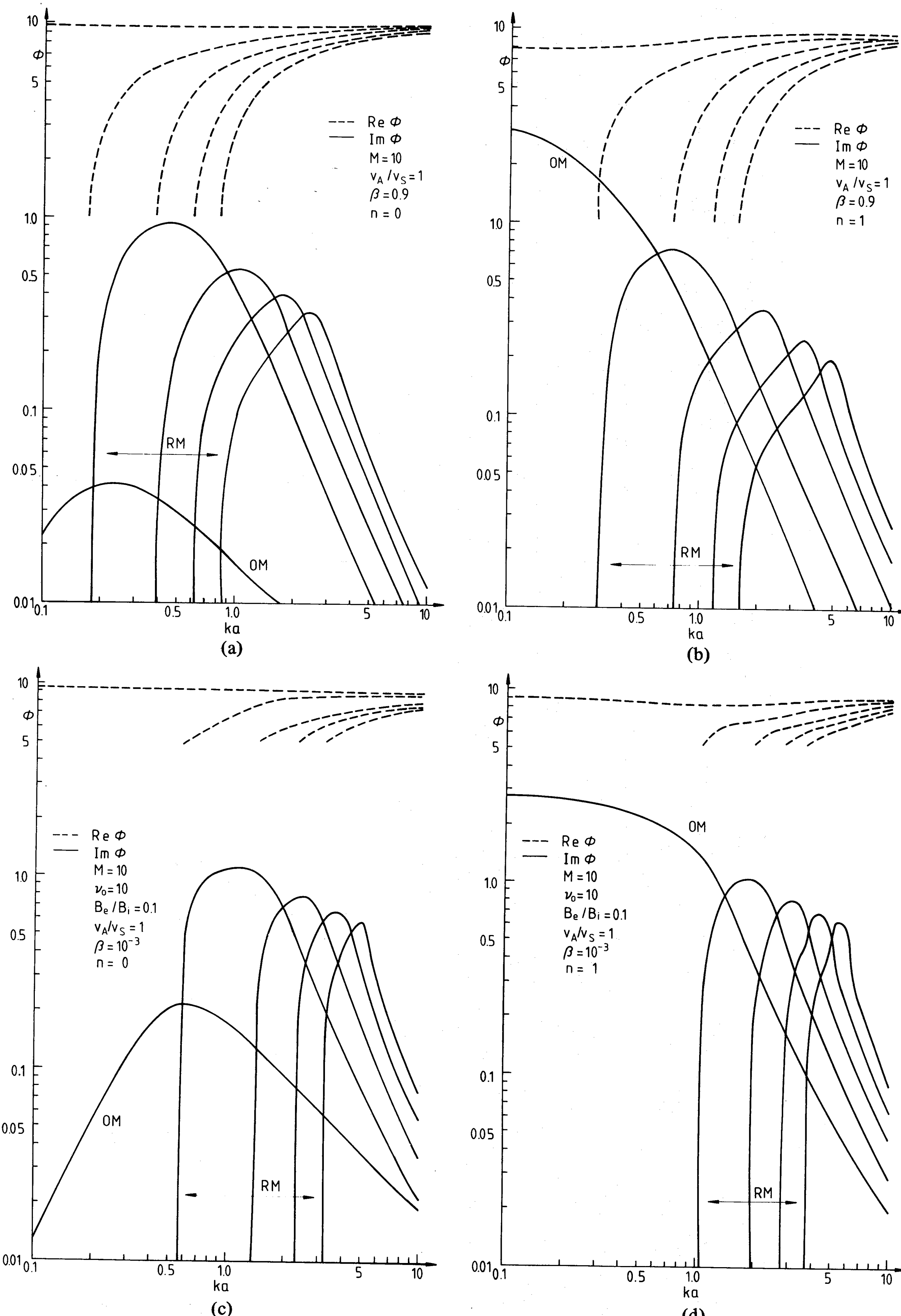

Figure 4. (a) Reϕ and Imϕ versus *ka* for unstable pinching modes in supersonic, relativistic flows. (b) Reϕ and Imϕ versus *ka* for unstable helical modes in supersonic relativistic flows. (c) Effects of density and magnetic field contrasts inside and outside the jet on pinching modes in supersonic flows. (d) Effects of density and magnetic field contrasts inside and outside the jet on helical modes in supersonic flows.

Table 1. Instability time-scales for supersonic flows in units of jet crossing-time $(\delta\tau_c)^{-1}$. The plane boundary results are from Paper I with $R = |k_\perp/k_\parallel|$; in this last case the non-dimensional values have been measured in terms of a scale distance $2a$, i.e. they give the instability e-folding time in terms of the same crossing-time as for jets.

Cylindrical jet							Plane boundary				
M	$ka = 0.1$		$ka = 1$		$ka = 10$		M	$ka = 1$		$ka = 10$	
	$n = 0$	$n = 1$	$n = 0$	$n = 1$	$n = 0$	$n = 1$		$R = 0$	$R = 10$	$R = 0$	$R = 10$
2.5	6.4×10^3	3.8	13.8	4	2.5	2.2					
5	9.6×10^2	9.2	6.0	4.2	1.4	1.4	5	∞	9.0	∞	0.9
10	2.2×10^2	5.0	2.2	2.2	1.0	0.9	10	∞	6.6	∞	0.5

Obviously, unstable modes are typically magnetosonic perturbations, and their phase velocity is $V_{\rm ph} \sim U_0$, i.e. they are dragged along by the flow at approximately the same speed. RMs have smaller phase velocities as they correspond to signals following non-rectilinear paths and reflected at the walls.

Concerning the growth rates, numerical results show that, almost independently of the physical parameters, supersonic flows are unstable especially to wavelengths of the order of the jet circumference, $ka \sim 1$ or $\lambda \sim 2\pi a$. The maximum growth rates are typically $\delta \sim 2(ka)\,{\rm Im}\,\phi/\tau_c$, and higher than the estimates that could be made from the plane vortex-sheet case. We give in Table 1 such a comparison in terms of $(\delta\tau_c)^{-1}$, the instability time-scale in units of the jet crossing-time. The plane vortex-sheet data with $R = |k_\perp/k_\parallel| = 0$ may be compared to pinching modes, and those with $R = 10$ to helical modes; we allowed extrapolation to a minimum $ka \sim 1$. It is clear that, contrary to the predictions of Paper I, pinching modes are always as unstable as helical and fluting modes, at least for $M \gtrsim 5$; although (for the same n) modes with larger ka have faster growths, the difference is never as wide as in the plane boundary case, so that long wavelengths have a chance to be excited together with shorter ones. This new trend of the solutions is obviously connected with the branch of RMs.

Although in Paper I the maximum growth rate was limited to the range $M|k_\perp/k_\parallel| \simeq 1.5$–$2$, this new branch always allows larger (or at least comparable) growth for $ka \gtrsim 1$ in supersonic flows, independently of the direction of the wavevector, i.e. both for pinching and helical or fluting modes. This is true also in the relativistic flow regime, and one must face the result that any jet is essentially unstable to Kelvin–Helmholtz instability, especially in the range of wavelengths that can be connected with observations (see next section).

3.7 TRANSVERSE DEVELOPMENT OF UNSTABLE MODES

In order to understand how and to what extent unstable modes perturb the flow, we must analyse their radial amplitude distribution. For this we recall that the dispersion relation (2) was obtained by expressing $g(r)$ in (1) in terms of transcendental cylindrical functions:

$$g(r) \propto \sum_n H_n^{(1)}(kr\Delta_e)$$

outside the jet, and

$$g(r) \propto \sum_n J_n(kr\Delta_i)$$

inside the jet. Correspondingly, the external amplitude distribution decreases outwards $\propto \exp\{-kr\,{\rm Im}\,\Delta_e\}/(kr\,{\rm Im}\,\Delta_e)^{1/2}$, apart from a slight dependence on the azimuthal wavenumber n; the internal distribution is a more complicated function, strongly dependent on n

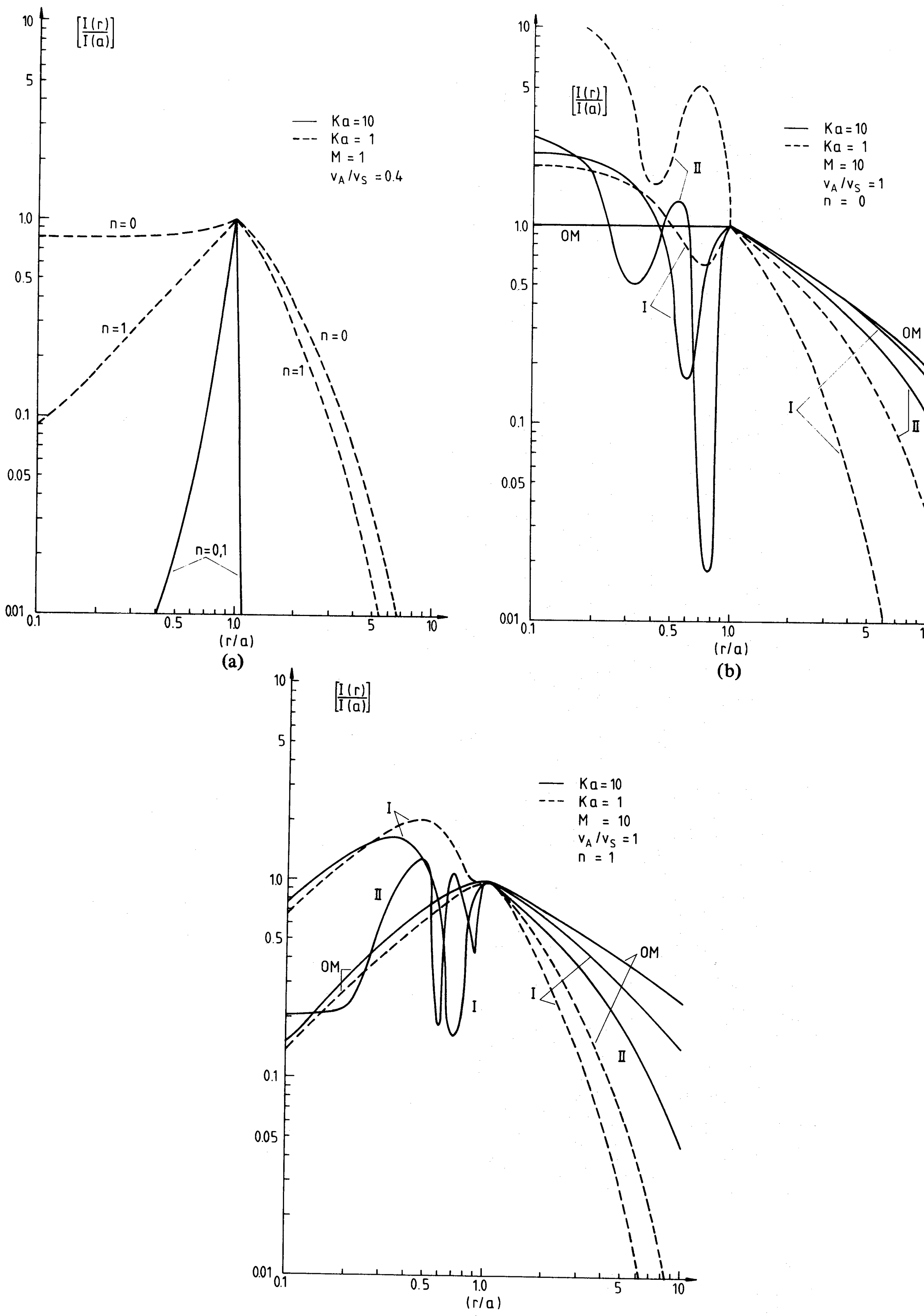

Figure 5. Radial amplitude distribution of unstable modes; the moduli of eigenfunctions inside ($r/a < 1$) and outside ($r/a > 1$) the jet are plotted, as normalized to their amplitude at the contact discontinuity ($r = a$). (a) Pinching and helical modes in transonic flows. (b) Pinching modes in supersonic flows, ordinary modes and two reflection modes. (c) Helical modes in supersonic modes, ordinary modes and two reflection modes.

and the mode considered, i.e. OM or RM. In Fig. 5 we give plots of the moduli of the eigenfunctions, $|\mathrm{Im}\,(kr\Delta_i)|$ and $|H_n^{(1)}\,(kr\Delta_e)|$, normalized to the perturbation at the cylinder wall $r=a$; such a modulus gives a measure of the energy distribution of the eigenmodes. The typical solutions in Fig. 5 indicate the following features:

(i) In subsonic and transonic flows with $M \lesssim 1$, since $\mathrm{Im}\,\Delta_{i,e} \sim 1$, both external and internal energy distributions are strongly concentrated at the cylinder walls for $ka \gg 1$; whereas, for large λs, the external cut-off is much less severe and the internal distribution depends on n: pinching modes perturb all the flow, and helical-mode perturbations decrease down to ~ 10 per cent at the axis.

(ii) In supersonic flows, the pattern is complicated by the onset of the reflection branch and by the fact that $\Delta_{i,e}$ are functions of ϕ; from Fig. 5(b) and (c) one can see, however, that all modes perturb the whole body of the jet: in addition the RMs decay faster outside and show an oscillatory energy distribution inside, the number of oscillations increasing for modes with growth rate peaked at larger ka.

In conclusion, instability in transonic flows is concentrated at the jet boundary; while, for supersonic flows, the whole jet is perturbed, with OMs corresponding to an almost constant energy distribution, and RMs to a largely inhomogeneous distribution, possibly separating narrow streams. Concerning the external extension of the perturbations, we also note that small wavelengths, $ka \gg 1$, survive up to ~ 10 times the jet radius, leading to the suggestion that a very extended halo forms around it, where non-linear dissipation effects may be expected to occur. Incidentally we note that these non-linear processes could also produce gradients of the physical quantities across the beam surface, requiring analysis of instabilities in shear layers.

We conclude this section with some remarks in connection with previous works.

It has been claimed that highly supersonic flows are stable with respect to all wavevectors, apart from those perpendicular to the vortex sheet which would not produce longitudinal structures in the flow. In fact, we have just shown that, in jets, RMs resonate at the boundaries, and for increasing Mach numbers involve longer wavelengths. Both pinching and helical modes are strongly enhanced, so that any flow must be considered unstable for $ka \sim 1$.

As a minor point, we note that Hardee (1979) has proposed the existence of modes with both positive and negative phase velocities for $ka \ll 1$. We incline to the view that negative phase velocities cannot exist, because in our calculations they would correspond to perturbation amplitudes increasing and diverging away from the jet.

4 Astrophysical implications

In the Introduction we argued that Kelvin–Helmholtz instabilities of axisymmetric flows may determine the structure and energetics of beams and jets in extended extragalactic radio-sources. In this framework, Hardee (1981) has attributed the 'wiggles' of radio jets in 3C 449 to the onset of helical modes of large wavelengths in (unmagnetized) flows; similarly pinching modes, again for $ka \sim 1$, could be responsible for the 'knots' observed in the M87 jet (Ferrari & Trussoni, in preparation).

In addition, Ferrari *et al.* (1978, 1979) have shown that these instabilities, although fast enough to generate perturbations of the flow pattern, actually reach a saturation stage before total disruption (or explosion) of the beam occurs. This is essentially due to fast and efficient local acceleration processes by MHD modes, transferring energy from the collimated flow to relativistic electrons, responsible for the radio brightness (Ferrari *et al.* 1979; Eilek 1979). Benford, Ferrari & Trussoni (1980) have then discussed in detail how, in this scheme, instabilities do not endanger the collimated energy supply to extended radio lobes, but instead represent a way to explain various morphological structures, for instance jets, bridges, flaring sources, etc. Have the refinements of the instability theory, that we have presented in this paper, any impact on such models?

A first effect is due to the presence of a magnetic field component along the flow velocity; then all modes are completely stable for sub-Alfvénic flows, and for mildly supersonic flows ($M \lesssim 2$) also, instabilities have low growth-rates. Long-wavelength pinching modes are stable in this range. Therefore in the region of jet formation – the nozzle of the Blandford & Rees model (1974) – where the plasma is probably relativistic ($V_S \sim c/\sqrt{3}$), instability is very weak because $M \sim \sqrt{3}$. Collimation is not perturbed so long as the parallel magnetic field is near equipartition ($V_A \sim V_S$).

Possibly 'wiggles' can be produced by $n = 1$ modes, but they cannot grow fast enough to destroy the beam. Knots are not expected to form as they should be correlated with pinching modes. Further out from the nozzle, fluting modes, or even the simple adiabatic expansion of the flow, transform the parallel field into transverse field.

For such a configuration we have shown how instabilities grow faster and may lead eventually to the destruction of beam collimation. This seems to be in agreement with the observations of polarization structures in 3C 449 (Perley, Willis & Scott 1979), NGC 315 (Bridle *et al.* 1979), 3C 31 (Fomalont *et al.* 1980).

The other relevant outcome of our calculations is the new branch of modes, for any azimuthal number, that arise for $M \gtrsim 2.5$. These modes have substantially faster growth rates, and appear to lead to the development of unstable modes especially in the region $ka \sim 1$. For large M, pinching modes are even faster than helical modes, and cannot be stabilized by equipartition magnetic fields. For modes $ka \ll 1$, helical modes prevail, while for $ka \gg 1$, pinching modes decay more slowly. A comparison of the instability growth-time with the typical source lifetime $\sim 10^7$ yr gives a lower limit for the wavenumbers that can affect a radio source beam:

$$ka \gtrsim 0.1 \frac{a_{\mathrm{kpc}}}{V_{S,8}} \frac{M}{\mathrm{Im}\,\phi},$$

where $V_{S,8}$ is given in $10^3\,\mathrm{km\,s^{-1}}$ units, a_{kpc} in kpc and a/V_S is the crossing time already defined. For the reflection modes, $\mathrm{Im}\,\phi \sim 1$, so that at $ka \sim 1$ they can grow even for largely supersonic flows.

The following scheme emerges in terms of the flow speed:

(1) Transonic flows, $M \simeq 2$–5, develop helical or fluting modes only, at least on large scales, because the RMs still have $ka \gg 1$. The behaviour of the OMs is generally that derived in previous papers (Ferrari *et al.* 1979; Hardee 1979).

(2) Supersonic flows, $M \gtrsim 5$, show fast instabilities also; and pinching modes have at least the same growth as helical ones.

In this scheme, slow jets would show 'wiggles', as subsonic jets do, but with faster growths. Conversely, pinching modes take over in fast jets at long wavelengths and their growth time is typically smaller than the source lifetime. Whether this means a disruption of the beam, cannot be evaluated in terms of a purely linear theory. However, numerical simulations (Nepveu 1980; Tajima & Leboeuf 1980) suggest that non-linear mode interactions are likely to saturate instabilities before one can detect any breaking.

In this respect we may also refer to a simple approach for estimating the non-linear evolution of perturbations. If the flowing streams have to be scattered with respect to the straight path induced by the initial collimation process, the transverse velocity displacement cannot exceed the sound speed without generating shocks. This means that the maximum scattering angle must be $\theta \lesssim 1/M$. For a perturbation of wavelength λ, this yields a maximum amplitude $\xi \sim \lambda/M$. These shocks can feed energy into thermal plasma and high-energy particles. This could observationally correspond to knots of emission in the jet boundary layer. Limb brightening is not necessarily implied, as this boundary is diffuse.

It is obvious that short wavelengths are saturated much earlier, and long wavelengths should become more evident. An observation that could favour this interpretation has been obtained in the Earth's magnetosphere by the satellite *ISEE-2*. It is well known how the interaction between the solar wind and the plasma of the magnetosphere leads to the dissipation of energy at the magnetosheath by KH instability, with generation of suprathermal particles and magnetosonic waves. On a different scale this process is similar to that we are suggesting for radio jets. Recently Hones *et al.* (1981) have measured the presence in the magnetotail of vortices having typical sizes of the order of the transverse dimensions of the tail itself. These vortices are possibly distributed homogeneously in the tail, while smaller-scale turbulence is confined within the magnetosheath. It is then likely that the non-linear evolution of the instability leads to a prevalence of long-wavelength perturbations. Of course, in radio sources such an effect might be much stronger and lead to the creation of shocks with faster dissipation. A study of these processes is beyond the aim of this paper. It is, however, important to have envisaged a way to allow instabilities to rise and support morphologies of the types observed. Reflection modes are highly relevant in determining these morphologies, as they are typical of the geometrical configuration considered.

We have also pointed out the formation of a boundary layer, because of the lateral development of a beam. This probably involves the generation of gradients, especially in the velocity distribution; such gradients could also be created by possible 'viscous' effects in the flow (Baan 1980; Nepveu 1980). We deal with the problem in a further paper of this series.

Acknowledgments

The authors thank C. Norman, G. Paschmann and P. Biermann for helpful discussions. AF also thanks the Max-Planck Institut für Physik und Astrophysik for hospitality during the final stages of this work.

The authors are grateful to the referee for pointing out typographical errors in the main formulae of the original version.

References

Baan, W. A., 1980. *Astrophys. J.*, **239**, 433.
Benford, G., Ferrari, A. & Trussoni, E., 1980. *Astrophys. J.*, **241**, 98.
Blandford, A. D. & Rees, M. J., 1974. *Mon. Not. R. astr. Soc.*, **169**, 395.
Bridle, A. H., Davies, M. M., Fomalont, E. B., Willis, A. G. & Strom, R. G., 1979. *Astrophys. J.*, **228**, L9.
Chakraborty, B. B. & Iyengar, H. K. S., 1975. *J. Plasma Phys.*, **14**, 443.
Chakraborty, B. B. & Iyengar, H. K. S., 1977. *J. Plasma Phys.*, **18**, 289.
Eilek, J. A., 1979. *Astrophys. J.*, **230**, 373.
Ershkovich, A. I. & Heller, A. B., 1977. *Astrophys. Space Sci.*, **48**, 365.
Ferrari, A., Trussoni, E. & Zaninetti, L., 1978. *Astr. Astrophys.*, **64**, 43.
Ferrari, A., Trussoni, E. & Zaninetti, L., 1979. *Astr. Astrophys.*, **79**, 190.
Ferrari, A., Trussoni, E. & Zaninetti, L., 1980. *Mon. Not. R. astr. Soc.*, **193**, 469 (Paper I).
Fomalont, E. B., Bridle, A. H., Willis, A. G. & Perley, R. A., 1980. *Astrophys. J.*, **237**, 418.

Gill, A. E., 1965. *Phys. Fluids,* **8,** 1428.
Hardee, P. E., 1979. *Astrophys. J.,* **234,** 47.
Hardee, P. E., 1981. *Astrophys. J.,* in press.
Hones, E. W., Birn, J., Bame, S. K., Asbridge, J. R., Paschmann, C., Schopke, N. & Haerendel, G., 1981. *J. Geophys. Res.,* submitted.
Lessen, M., Fox, J. A. & Zien, H. M., 1965. *J. Fluid Mech.,* **21,** 129.
Miles, J. W., 1957. *J. Acoust. Soc. Am.,* **29,** 226.
Nepveu, M., 1980. *Astr. Astrophys.,* **84,** 14.
Perley, R. A., Willis, A. G. & Scott, J. S., 1979. *Nature,* **281,** 437.
Ray, T. P., 1981. *Mon. Not. R. astr. Soc.,* **196,** 195.
Tajima, R. & Leboeuf, J. N., 1980. *Phys. Fluids,* **23,** 884.